Journal of Engineering and Applied Sciences 13 (11): 4156-4164, 2018
ISSN: 1816-949X

Mechanical and Temperature Stress Composite Material Pipes with Finite Length

[1]Emad Toma Karash, [2]Tymor Abed Alsttar Sediqer and [3]Nawal Abdul Hakeem Husain
[1]Department of Agricultural Mechanization Techniques,
[2]Department of Civil Techniques, [3]Department of Mechanical Techniques,
Northern Technical University, 00964 Erbil, Iraq

Abstract: The stress and strain condition of a multi-layer hollow cylinder of limited length under the effect of internal pressure and heat is confirmed on the basis of the classical theory of anisotropic body elasticity. The kinematic and static conditions of contact coordinating surfaces of neighboring layers are supposed ideal. By using a multi-layered nearby based on the theory of the layered composites, the solutions of temperature, displacements and mechanical thermal stresses in a functionally stepped circular hollow cylinder are obtainable in this research. The cylinder has finite length and is yielded to to axisymmetric mechanical and thermal loads. The values of the internal pressure and temperature vary sinusoid ally laterally the length of the cylinder. The results showed that, the increase in temperature on the outer surface of the composite pipe has a significant effect on its stress state. The maximum normal stresses in the longitudinal direction in the outer layer of duralumin increased by 59% with an increase in temperature of only 30 K and 57% in bearing layer of fiberglass. When analyzing the changes of normal stresses in the circumferential direction of the cylinder temperature rise 30 K marked decrease in these stresses of 6% in the outer layer and 2% in the carrier layer.

Key words: Stress, strain, fiberglass, finite length, composite pipe, outer

INTRODUCTION

Composite materials are still found in limited use, primarily in the high performance industries (automotive, aeronautical and marine) (Dasgupta and Huang, 1997; Jain and Mai, 1997; Tucker *et al*., 2001). This is due to a lack of knowledge and full understanding of the mechanisms governing composite materials. This is extremely true when dealing with thick composite parts as the majority of applications of composite materials are with thin laminates (and hence, the majority of analysis is centered on this).

In metallic structures, increases in thickness do not generally possess any serious implications, apart from part cost. In contrast, the increase in thickness of composite parts has serious implications which need to be considered. To compound this, these effects do not account for by the traditional methods of analysis for anisotropic materials.

Traditionally, composite analysis techniques tend to be based on the assumption of plane stress and are therefore only applicable to thin laminates. Possibly the most well-known of these techniques is Classical Lamination Plate Theory (CLPT) (Herakovich, 1997). Many researches have been approved out for thermo elastic problems of functionally arranged constructions (Obata and Noda, 1994; Tanigawa, 1999; Ootao and Tanigawa, 2000; Kim and Noda, 2002a, b). Kim and Noda (2002) studied the one-dimensional steady thermal stresses in a functionally arranged circular hollow cylinder and hollow sphere by using a agitation method. By introducing the theory of laminated composites but work (Jabbari *et al*., 2002) treated the three, three-dimensional passing thermal loading of functionally coordinated rectangular plates caused by partial heating was studied. Piezoelectric thermoelastic problems of piezoelectric plates and functionally prepared rectangular plates have been analyzed (Jabbari *et al*., 2003).

In this research we considered the steady thermoelasticity of a circular hollow cylinder with a finite functional configuration. The mechanical and thermomechanical loads spend on the cylinder are axisymmetric in the structural orientation and different in the axial orientation. In order to take out analytical solutions for temperature, displacement and stress for the two-dimensional thermoelastic problem, the cylinder should contain of n workable layers in the radial direction.

MATERIALS AND METHODS

Basic equations: When the circular hollow loaded is mounted on a cylindrical surface $r = r_a$ and $r = r_b$ stationary temperature leads $t_a(z)$ and $t_b(z)$ and uniformly

Corresponding Author: Emad Toma Karash, Department of Agricultural Mechanization Techniques,
Northern Technical University, 00964 Erbil, Iraq

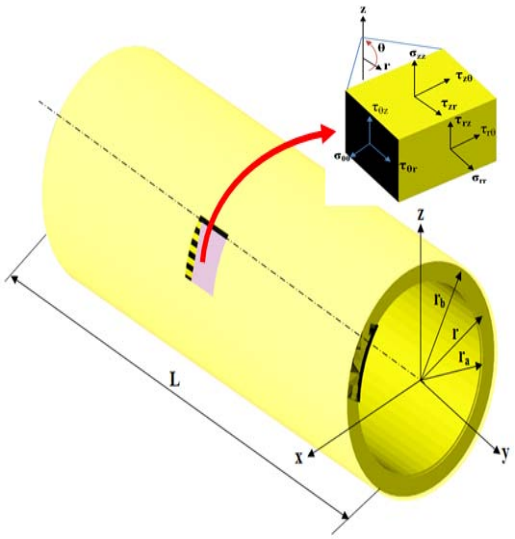

Fig. 1: Multilayer circular hollow cylinder of finite length

deal out lengthways the circumferential coordinate efforts q_a (z) and q_b (z). Directions of the axes of the cylindrical system coordinates are show in Fig. 1.

The stresses that arise in point of the cylinder undera the an act of an external load Fig. 1b. It is believed that the thermal load is specified in the personal cylindrical surfaces with respect to axisymmetric pressure the longitudinal axis of the cylinder. But their magnitude varies along meridian and based on the coordinate z. Moreover, the length of the cylinder is infinite 1 and it had free end bearing conditions. As well as in solving the problem effect of slip cylinder layers for each other in the longitudinal direction can be considered.

Based on the theory of anisotropic elastic body (Lekhnitskij, 1977) equilibrium equations, physical and geometric relationships were drawn in order to solve this case:

$$\left[B_r^i\right]=\begin{bmatrix} b_{11}^i & b_{12}^i & b_{13}^i & 0 & 0 & 0\\ 0 & b_{22}^i & b_{23}^i & 0 & 0 & 0\\ 0 & 0 & b_{33}^i & 0 & 0 & 0\\ 0 & 0 & 0 & b_{44}^i & 0 & 0\\ 0 & 0 & 0 & 0 & b_{55}^i & 0\\ 0 & 0 & 0 & 0 & 0 & b_{66}^i \end{bmatrix}=\begin{bmatrix} \frac{1}{E_r^i} & -\frac{\nu_{\theta r}^i}{E_\theta^i} & -\frac{\nu_{zr}^i}{E_z^i} & 0 & 0 & 0\\ -\frac{\nu_{r\theta}^i}{E_r^i} & \frac{1}{E_\theta^i} & -\frac{\nu_{z\theta}^i}{E_z^i} & 0 & 0 & 0\\ -\frac{\nu_{rz}^i}{E_r^i} & -\frac{\nu_{\theta z}^i}{E_\theta^i} & \frac{1}{E_z^i} & 0 & 0 & 0\\ 0 & 0 & 0 & \frac{1}{G_{\theta z}^i} & 0 & 0\\ 0 & 0 & 0 & 0 & \frac{1}{G_{rz}^i} & 0\\ 0 & 0 & 0 & 0 & 0 & \frac{1}{G_{r\theta}^i} \end{bmatrix}$$

Geometric equations: With a cylindrical coordinate system r, θ, z and specifying the direction of the x-axis, measured at an angle θ Fig. 1a, the following physical relationships i-the can be written for the contrast of the cylinder layer derived from layer:

$$\left\{\varepsilon_r^i\right\}=\left[B_r^i\right].\left\{\sigma_r^i\right\}+\left\{\alpha_r^i.\Delta t\right\}\ (i=1,2,...,N) \qquad (1)$$

Where:

$$\left\{\sigma_r^i\right\}=\begin{Bmatrix}\sigma_r^i\\ \sigma_\theta^i\\ \sigma_z^i\\ \tau_{\theta z}^i\\ \tau_{rz}^i\\ \tau_{r\theta}^i\end{Bmatrix},\ \left\{\varepsilon_r^i\right\}=\begin{Bmatrix}\varepsilon_r^i\\ \varepsilon_\theta^i\\ \varepsilon_z^i\\ \gamma_{\theta z}^i\\ \gamma_{rz}^i\\ \gamma_{r\theta}^i\end{Bmatrix},\ \left\{\alpha_r^i\Delta t\right\}=\begin{Bmatrix}\alpha_r^i\Delta t\\ \alpha_\theta^i\Delta t\\ \alpha_z^i\Delta t\\ 0\\ 0\\ 0\end{Bmatrix}$$

Matrix columns stress-strain state with thermal strains and the coefficient matrix yielding $[B_r^i]$. respectively. Here, $[E_r^i, E_\theta^i, E_z^i]$ are the moduli of elasticity $[G_{\theta z}^i, G_{r\theta}^i, G_{rz}^i]$ in the radial, circumferential and longitudinal directions, shear moduli in the planes $[\theta_{oz}, r_{oz}, r_{o\theta}]$, respectively, $[\upsilon_{kj}^i (k, j = r, \theta, z)]$ -Poisson's ratios, $[\alpha_j^i (j = r, \theta, z)]$ -coefficient of Linear thermal amplification in cylindrical axis directions, [Δt] temperature change on the front surface of the cylinder, N-number of layers of the cylinder. Solving equation system 1, it is simple to detection the following physical relationships:

$$\left\{\sigma_r^i\right\}=\left[A_r^i\right]\left\{\varepsilon_r^i\right\}-\left\{\alpha_r^i\Delta t\right\} \qquad (2)$$

Where:

$$\left[A_r^i\right]=\begin{bmatrix} a_{11}^i & a_{12}^i & a_{13}^i & 0 & 0 & 0\\ 0 & a_{22}^i & a_{23}^i & 0 & 0 & 0\\ 0 & 0 & a_{33}^i & 0 & 0 & 0\\ 0 & 0 & 0 & a_{44}^i & 0 & 0\\ 0 & 0 & 0 & 0 & a_{55}^i & 0\\ 0 & 0 & 0 & 0 & 0 & a_{66}^i \end{bmatrix}$$

$$\left[\alpha_r^i\Delta t\right]=\begin{bmatrix}\left(\alpha_{11}^i+\alpha_{12}^i+\alpha_{13}^i\right)\alpha_r^i\Delta t\\ \left(\alpha_{21}^i+\alpha_{22}^i+\alpha_{23}^i\right)\alpha_\theta^i\Delta t\\ \left(\alpha_{31}^i+\alpha_{32}^i+\alpha_{33}^i\right)\alpha_z^i\Delta t\\ 0\\ 0\\ 0\end{bmatrix}$$

Here are the coefficients of the stiffness matrix $[A_r^i]$ determined by the expressions:

$$a_{11}^i = \left[b_{22}^i b_{33}^i - \left(b_{23}^i\right)^2 \right].\Delta^{-1},$$
$$a_{22}^i = \left[b_{11}^i b_{33}^i - \left(b_{13}^i\right)^2 \right].\Delta^{-1},$$
$$a_{33}^i = \left[b_{11}^i b_{22}^i - \left(b_{12}^i\right)^2 \right].\Delta^{-1},$$
$$a_{12}^i = \left[b_{13}^i b_{23}^i - b_{12}^i b_{33}^i \right].\Delta^{-1},$$
$$a_{13}^i = \left[b_{12}^i b_{23}^i - b_{22}^i b_{13}^i \right]. \Delta^{-1},$$
$$a_{23}^i = \left[b_{12}^i b_{13}^i - b_{11}^i b_{23}^i \right]. \Delta^{-1},$$
$$\Delta = b_{11}^i b_{22}^i b_{33}^i + b_{12}^i b_{23}^i b_{31}^i + b_{21}^i b_{32}^i b_{13}^i - b_{13}^i b_{22}^i b_{31}^i + b_{21}^i b_{12}^i b_{33}^i + b_{11}^i b_{32}^i b_{23}^i$$
$$a_{44}^i = \frac{1}{b_{44}^i},\ a_{55}^i = \frac{1}{b_{55}^i},\ a_{66}^i = \frac{1}{b_{66}^i}$$

Geometric relations:

$$\varepsilon_r^i = \frac{\partial u_r^i}{\partial r}\ \varepsilon_\theta^i = \frac{1}{r}\frac{\partial u_\theta^i}{\partial \theta} + \frac{u_r^i}{r}\ \varepsilon_z^i = \frac{\partial u_z^i}{\partial z},$$
$$\gamma_{\theta z}^i = \frac{\partial u_\theta^i}{\partial z} + \frac{1}{r}\frac{\partial u_z^i}{\partial \theta}\ \gamma_{rz}^i = \frac{\partial u_z^i}{\partial r} + \frac{\partial u_r^i}{\partial z}, \quad (3)$$
$$\gamma_{r\theta}^i = \frac{\partial u_r^i}{\partial \theta} + \frac{\partial u_\theta^i}{\partial r} - \frac{u_\theta^i}{r} \quad (i = 1, 2, ..., N)$$

where, u_r^i, u_θ^i, u_z^i move in the radial, circumferential and longitudinal direction of the I-the layer orthotropic cylinder ($r_i \langle r \langle r_{i+1}$), respectively.

The problem in the preparation of the axisymmetric about the axis z, u_θ^i displacement does not change in the peripheral direction. Therefore, the Eq. 3 can be rewritten as follows:

$$\varepsilon_r^i = \frac{\partial u_r^i}{\partial r}\ \varepsilon_\theta^i = \frac{\partial u_r^i}{r}\ \varepsilon_z^i = \frac{\partial u_z^i}{\partial z}\ \gamma_{\theta z}^i = 0$$
$$\gamma_{rz}^i = \frac{\partial u_z^i}{\partial r} + \frac{\partial u_r^i}{\partial z}\ \gamma_{r\theta}^i = \frac{u_\theta^i}{r} \quad (i = 1, 2, ..., N) \quad (4)$$

Equilibrium equations: When formulating a two-dimensional axisymmetric equation of equilibrium problem the traditional theory of anomaly elasticity (Tucker *et al*., 2001) takes viewers:

$$\frac{\partial \sigma_r^i}{\partial r} + \frac{\partial \tau_{rz}^i}{\partial z} + \frac{\sigma_r^i - \sigma_\theta^i}{r} = 0,\ \frac{\partial \tau_{rz}^i}{\partial r} + \frac{\partial \sigma_z^i}{\partial z} + \frac{\partial \tau_{rz}^i}{r} = 0 \quad (5)$$

Complemented third heat equation by two equilibrium Eq. 6:

$$\left(\frac{\sigma^2}{\partial r^2} + \frac{1}{r}\frac{\partial}{\partial r} + \frac{\partial^2}{\partial z^2} \right) t^i = 0 \quad (6)$$

In order to solve this item for a system self-possessed of three partial differential Eq. 5 and 6, we should set the boundary conditions at the ends and front surfaces cylinder and the conditions of contact for join surfaces neigsdfhboring layers.

Boundary conditions: In the face of the end cylinder:

$$u_r^i(r, 0) = 0\ ,\ \sigma_z^i(r, 0) = \tau_{rz}^i(r, 0) = 0,$$
$$u_r^i(r, 1) = 0,\ \sigma_z^i(r,1) = \tau_{rz}^i(r, 1) = 0,$$
$$\sigma_r^1(r_a, z) = q_a(z),\ \tau_{rz}^1(r_a, z) = 0,$$
$$\sigma_r^N(r_b, z) = q_b(z),\ \tau_{rz}^N(r_b, z) = 0, \quad (7)$$
$$t^i(r, 0) = t^i(r, 1) = 0 \quad (i = 1, 2, ..., N),$$
$$t^1(r_a, z) = t_a(z),\ t^N(r_b, z) = t_b(z)$$

On the join surfaces of neighboring layers:

$$\sigma_r^{i-1}(r_i, z) = \sigma_r^i(r_i, z),\ \tau_{rz}^{i-1}(r_i, z) = \tau_{rz}^i(r_i, z) u_r^{i-1}(r_i, z) =$$
$$u_r^i(r_i, z),\ u_z^{i-1}(r_i, z) - u_z^i(r_i, z) = K.\tau_{rz}^i(r_i, z) t^{i-1}(r_i, z) = \quad (8)$$
$$t^i(r_i, z),\ \lambda^{i-1}\frac{\partial t^{i-1}(r_i, z)}{\partial r} = \lambda^i \frac{\partial t^i(r_i, z)}{\partial r}\ (i = 1, 2, ..., N)$$

In the final Eq. 8 factor λ_i corresponds to a factor thermal accessibility of th e i-th layer. Equation 8 holds two options: the 1/K(i) = 0 is elastic slip neighboring layers each proportion of each other along intermarry surfaces while k_i-Communication perfection.

The dimensionless parameters: To simplify data input and synthesis numerical results, following (Herakovich, 1997), enter the next dimensionless quantities:

$$R = \frac{r}{r_b},\ R_a = \frac{r_a}{r_b},\ R_b = \frac{r_b}{r_b} = 1,\ Z = \frac{z}{r_b},$$
$$L = \frac{1}{r_b},\ A_{kl}^i = \frac{a_{kl}^i}{E_o},\ \Gamma_k^i = \frac{\gamma_k^i}{\alpha_o E_o},$$
$$T^i = \frac{t^i}{t_o},\ \Lambda^i = \frac{\lambda^i}{\lambda_o},\ U_r^i = \frac{u_r^i}{A\alpha_o E_o r_b},\ U_z^i = \frac{u_z^i}{\alpha_o E_o r_b},$$
$$S_r^i = \frac{\sigma_r^i}{\alpha_o E_o t_o},\ S_z^i = \frac{\sigma_z^i}{\alpha_o E_o t_o},\ S_\theta^i = \frac{\sigma_\theta^i}{\alpha_o E_o t_o}, \quad (9)$$
$$TU_{rz}^i = \frac{\tau_{rz}^i}{\alpha_o E_o t_o},\ Q_a(z) = \frac{q_a(z)}{\alpha_o E_o t_o},\ Q_b(z) = \frac{q_b(z)}{\alpha_o K_o t_o},$$
$$T_a(z) = \frac{t_a(z)}{t_o},\ T_b(z) = \frac{t_b(z)}{t_o}$$

where, E_0, λ_0 and α_0-modulus of elasticity, thermal conductivity and coefficient of thermal linear amplification of the reference material, t_0-indication temperature of the cylinder.

Equations of the boundary condition: Compensating Eq. 4 and 5 as well as given the dimensionless parameters introduced above, we can get:

$$\left[A_{11}^{i}\left(\frac{\partial^2}{\partial R^2}+\frac{1}{R}\frac{\partial}{\partial R}\right)-\frac{A_{22}^{i}}{R^2}+A_{55}^{i}\frac{\partial^2}{\partial Z^2}\right]U_r^i+$$
$$\left[\left(A_{13}^{i}+A_{55}^{i}\right)\frac{\partial^2}{\partial R\,\partial Z}+\left(A_{13}^{i}-A_{23}^{i}\right)\frac{\partial}{\partial Z}\right]U_z^i=\Gamma_r^i\frac{\partial T^i}{\partial R}$$
$$\left[\left(A_{13}^{i}+A_{55}^{i}\right)\frac{\partial^2}{\partial R\,\partial Z}+\left(A_{23}^{i}-A_{55}^{i}\right)\frac{1}{R}\frac{\partial}{\partial Z}\right]U_r^i+ \quad (10)$$
$$\left[\left[A_{55}^{i}\left(\frac{\partial^2}{\partial R^2}+\frac{1}{R}\frac{\partial}{\partial R}\right)+A_{33}^{i}\frac{\partial^2}{\partial Z^2}\right]\right]U_z^i=\Gamma_r^i\frac{\partial T^i}{\partial Z}$$
$$\left(\frac{\partial^2}{\partial R^2}+\frac{1}{R}\frac{\partial}{\partial R}\right)T^i+\frac{\partial^2 T^2}{\partial Z^2}=0$$

The boundary Eq. 7 and 8 recorded using dimensionless parameters Eq. 9 takes the form: At the ends of the cylinder faces:

$$\begin{aligned}
&U_r^i(R,0)=0,\ S_z^i(R,0)=TU_{rz}^i(R,0)=0\\
&U_r^i(R,0)=0,\ S_z^i(R,1)=TU_{rz}^i(R,1)=0\\
&S_r^1(R_a,z)=Q_a(z),\ TU_{rz}^1(R_a,z)=0\\
&S_r^N(R_b,z)=Q_b(z),\ TU_{rz}^N(R_b,z)=0\\
&T^i(R,0)=T^i(R,1)=0\ (i=1,2,...,N),\\
&T_r^1(R_a,z)=T_a(z),\ T^N(R_b,z)=T_b(z)
\end{aligned} \quad (11)$$

On the overlapping surfaces of adjacent laers:

$$\begin{aligned}
&S_r^{i-1}(R_i,z)=S_r^i(R_i,z),\ TU_{rz}^i(R_i,z)=\\
&TU_{rz}^i(R_i,z),\ U_r^{i-1}(R_i,z)=U_r^i(R_i,z),\\
&U_{rz}^i(R_i,z)-U_z^i(R_i,z)=K.TU_{rz}^i(R_i,z)\\
&T^{i-1}(R_i,z)=T^i(R_i,z),\ \Lambda^{i-1}\frac{\partial T^{i-1}(R_i,z)}{\partial R}=\\
&\Lambda^i\frac{\partial T^i(R_i,z)}{\partial R}\quad (i=1,2,...,N)
\end{aligned} \quad (12)$$

Algorithm solves boundary value problems: Solution of the boundary Eq. 10-12 towards the longitudinal axis cylinder found in the procedure of trigonometric sequence:

$$\begin{aligned}
U_r^i(R,Z)&=\sum_{n=1}^{\infty}\Phi_n^i(R).\sin(\beta Z)\\
U_z^i(R,Z)&=\sum_{n=1}^{\infty}\Psi_n^i(R).\cos(\beta Z)\\
T_r^i(R,Z)&=\sum_{n=1}^{\infty}F_n^i(R).\sin(\beta Z)
\end{aligned} \quad (13)$$

where, $\beta = n\pi X_b/L$ Eq. 13 satisfy the circumstances of allowed backup at the ends of the cylinder. To compensate Eq. 13 by Eq. 10, we get the following:

$$\left[A_{11}^{i}\left(\frac{d^2}{dR^2}+\frac{1}{R}\frac{d}{dR}\right)-\frac{A_{22}^{i}}{R^2}+A_{55}^{i}\beta^2\right]\Phi_n^i(R)+$$
$$\left[\left(A_{13}^{i}+A_{55}^{i}\right)\beta\frac{d}{dR}+\left(A_{13}^{i}-A_{23}^{i}\right)\frac{\beta}{R}\right]\Psi_z^i(R)=$$
$$\Gamma_r^i\frac{dT_n^i(R)}{dR}\left[\left(A_{13}^{i}+A_{55}^{i}\right)\beta\frac{d}{dR}+\left(A_{23}^{i}-A_{55}^{i}\right)\frac{\beta}{R}\right] \quad (14)$$
$$\Phi_n^i(R)+\left[\left[A_{55}^{i}\left(\frac{d^2}{dR^2}+\frac{1}{R}\frac{d}{dR}\right)+A_{33}^{i}\beta^2\right]\right]$$
$$\Psi_n^i(R)=\Gamma_r^iF_n^i(R)\left[\left(\frac{d^2}{dR^2}+\frac{1}{R}\frac{d}{dR}\right)-\beta^2\right]F_n^i(R)=0$$

A similar scheme and boundary conditions are converted Eq. 11 and 12. At the end and faces of the cylinder:

$$\begin{aligned}
&A_{11}^1\frac{d\Phi_n^1(R_a)}{dR}+A_{12}^1\frac{\Phi_n^1(R_a)}{R}-\beta A_{13}^1\Psi_n^1(R_a)=Q_{an}\\
&A_{11}^N\frac{d\Phi_n^N(R_b)}{dR}+A_{12}^N\frac{\Phi_n^N(R_a)}{dR}=0A_{11}^N\frac{d\Phi_n^N(R_b)}{dR}+\\
&A_{12}^N\frac{\Phi_n^N(R_b)}{R}-\beta A_{13}^N\Psi_n^N(R_b)=Q_{bn}\ \beta\Phi_n^N(R_b)+\\
&\frac{d\Psi_n^N(R_b)}{dR}=0,\ F_n^1(R_a)=T_{an},\quad F_n^N(R_b)=T_{bn}
\end{aligned} \quad (15)$$

On the intermarry surfaces of neighboring layers:

$$A_{11}^{i-1}\frac{d\Phi_n^{i-1}(R^i)}{dR}+A_{12}^{i-1}\frac{\Phi_n^{i-1}(R^i)}{R}-\beta A_{13}^{i-1}\Psi_n^{i-1}(R^i)=$$
$$A_{11}^{i}\frac{d\Phi_n^{i-1}(R^i)}{dR}+A_{12}^{i}\frac{\Phi_n^{i-1}(R^i)}{dR}-\beta A_{13}^{i}\Psi_n^{i}(R^i)\beta\Phi_n^{i-1}(R^i)+$$
$$\frac{d\Psi_n^{i-1}(R^i)}{dR}=\beta\Phi_n^i(R^i)+\frac{d\Psi_n^i(R^i)}{dR},\ \Phi_n^{i-1}(R^i)=\Phi_n^{i-1}(R^i)$$
$$\Psi_n^{i-1}(R^i)-\Psi_n^i(R^i)=K\left[\beta\Phi_n^i(R^i)+\frac{d\Psi_n^i(R^i)}{dR}\right]$$
$$F_n^{i-1}(R^i)=F_n^{i-1}(R^i),\ \Lambda^{i-1}\frac{dF_n^N(R^i)}{dR}=\Lambda^i\frac{dF_n^i(R^i)}{dR}$$

Where:

$$Q_{an}=\frac{1}{L}\int_0^{2L}Q_a(Z)\sin(\beta Z)dZ,\ Q_{bn}=\frac{1}{L}\int_0^{2L}Q_b(Z)\sin(\beta Z)dZ \quad (16)$$
$$T_{an}=\frac{1}{L}\int_0^{2L}T_a(Z)\sin(\beta Z)dZ,\ T_{bn}=\frac{1}{L}\int_0^{2L}T_b(Z)\sin(\beta Z)dZ$$

It is believed to function in the radial direction $\Phi_n^i(R^i), \Psi_n^i(R^i), F_n^i(R^i)$ continuous with respect to the thickness of the i-th layer, then using the Taylor series they can be written as:

$$\Phi_n^i(R) = \sum_{k=0}^{\infty} C_k^i (R\text{-}1)^k, \quad \Psi_n^i(R) = \sum_{k=0}^{\infty} B_k^i (R\text{-}1)^k, \; F_n^i(R) = \sum_{k=0}^{\infty} D_k^i (R\text{-}1)^k \tag{17}$$

Substituting Eq. 17 into Eq. 15 and equally coefficients $(R\text{-}1)^k$ to zero, we can simply get the following Eq. 18:

$$B_{k+2}^i = \frac{1}{(k+2)(k+1)} \left[\begin{array}{l} -(k+1) B_{k+1}^i + \frac{\beta^2 A_{33}^i}{A_{55}^i} B_k^i - (k+1) \\ \beta \frac{A_{13}^i + A_{55}^i}{A_{55}^i} C_{k+1}^i - \beta \frac{A_{55}^i - A_{23}^i}{A_{55}^i} C_k^i + \frac{\Gamma_r^i}{A_{55}^i} D_K^i \end{array} \right]$$

$$D_{k+2}^i = \frac{1}{(k+2)(k+1)} \left[-(k+1) D_{k+1}^i + \beta^2 \; {}_k^i \right] \tag{18}$$

From the recurrence Eq. 18, it follows that all the coefficients C_k^i, B_k^i and D_k can be expressed through C_o^i, C_1^i, B_o^i, B_1^i, D_o^i, D_1^i, when k>1. Then the system of Eq. 15 can be written in compact form:

$$\psi_n^i(R) = \sum_{k=0}^{\infty} \left[\begin{array}{l} g_b^i(k,1) C_o^i + g_b^i(k,2) + g_b^i(k,3) B_o^i + \\ g_b^i(k,4) B_1^i + g_b^i(k,5) D_o^i + g_b^i(k,6) D_1^i \end{array} \right] (R\text{-}1)^k,$$

$$\Phi_n^i(R) = \sum_{h=0}^{\infty} \left[\begin{array}{l} g_c^i(k,1) C_o^i + g_c^i(k,2) + g_c^i(k,3) B_o^i + \\ g_c^i(k,4) B_1^i + g_c^i(k,5) D_o^i + g_c^i(k,6) D_1^i \end{array} \right] (R\text{-}1)^k,$$

$$F_n^i(R) = \sum_{h=0}^{\infty} \left[\begin{array}{l} g_d^i(k,1) C_o^i + g_d^i(k,2) + g_d^i(k,3) B_o^i + \\ g_d^i(k,4) B_1^i + g_d^i(k,5) D_o^i + g_d^i(k,6) D_1^i \end{array} \right] (R\text{-}1)^k \tag{19}$$

where, $g_b^i(k,0), g_c^i(k,j), g_d^i((k,j)$ constants determined using the recurrence Eq. 19. Unknown constants C_o^i, C_1^i, B_0^i, B_1^i, D_o^i, the number of which is determined by the number of discrete words cylinder N are found by substituting Eq. 19 into the boundary Eq. 15 and 16. Obtained with the linear algebraic system of equations contains 6N unidentified constants.

After decisive the value of the Eq. 19 and substituting them into the specific solutions Eq. 13, it is easy with the help of geometrical and physical relations presented above to solve the problem of the value of flexible thermal limits.

RESULTS AND DISCUSSION

Geometric parameters of multilayer circular hollow cylinder $r_a = 0.148$ m, $r_b = 0.18$ m and $l = 1$ m. The reference temperature, modulus of elasticity and coefficient equal to: $T_0 = 50$ K, $E_0 = 40$ GPa and $a_0 = 7.0 \cdot 10^{-5} K^{-1}$. Thermal stress on the inside and the outer surface and internal and external pressure are defined as follows where:

$$T_a(z) = 0, \quad T_b(z) = \Delta T . \sin\left(\frac{\pi z}{1}\right)$$

$$q_a(z) = q_o . \sin\left(\frac{\pi z}{1}\right), \quad q_b(z) = 0$$

$$q0 = 50 \text{ MPa}, \; \Delta T = 50 \text{ K}; 80 \text{ K}$$

The cylinder consists of 4 layers: A solid high density polyethylene pressure (h = 4 mm) E = 260 MPa, $\lambda = 0.4$, $\alpha = 0.44$ W/m·K, $\alpha = 20 \cdot 10^{-5} K^{-1}$; Fiberglass (h = 20 mm), $\lambda = 0.4$ W/m·K, $\alpha = 4\text{-}7 \cdot 10^{-5} K^{-1}$; Penovinilplast (h = 4 mm) E = 83 MPa, v = 0.33, $\lambda = 0.4$ W/m·K, $\alpha = 15 \cdot 10^{-5} K^{-1}$; Duralumin (h = 4 mm) E = 71GPa, v = 0.31, $\lambda = 160$ W/m·K, $\alpha = 2.3 \cdot 10^{-5} K^{-1}$. For the first-fourth layers made of a resilient isotropic material, the following relations:

$$E_z = E_\theta = E_r = E, \; G_{\theta z} = G_{r\theta} = G_{rz} = G,$$

$$\nu_{z\theta} = \nu_{zr} = \nu_{\theta r} = \nu_{\theta z} = \nu_{rz} = \nu_{r\theta} = \nu, \; G = \frac{E}{2(1+\nu)}$$

Flexible properties were identified in the fiberglass method (Dasgupta and Huang, 1997). The modulus of elasticityof E_B, modulus of rigidity G_v and Poisson's ratio v_B wound bars, recruited from aluminoboro silicate yarns, $E_B = 55.000$ MPa, $G_B = 22000$ MPa and $v_B = 0.25$. The template fiberglass epoxy resin was used with the following elastic parameters: $E_B = 3550$ MPa, $G_B = 1270$ MPa and $v_B = 0.4$.

B Each 0.25 mm thick monolayer volume engaged ribbons (70%) of the whole volume. Technical keep under review the multilayer fiberglass is summarized in Table 1. Analysis of theoretical results can be observed in Fig. 2-12, the following can be seen: the maximum normal stresses in the longitudinal direction Fig. 8 in the outer layer of duralumin increased by 59% with an increase in

Table 1: Elastic characteristics f fiberglass

Reinforcement arrangement	E (MPa)	G (MPa)	V_{ij}	V_{ij}
$[0°_4/-75°/0°_2\text{-}75°/$	$E_z = 23800$	$G_{\theta z} = 23800$	$G_{r\theta} = 23800$	$V_{\theta z} = 23800$
$75°/0°_2/\text{-}75°/0°_2$	$E_\theta = 33500$	$G_{rz} = 33500$	$G_{zr} = 33500$	$V_{rz} = 23800$
	$E_r = 23870$	$G_{r\theta} = 23870$	$G_{\theta r} = 23870$	$V_{r\theta} = 23800$

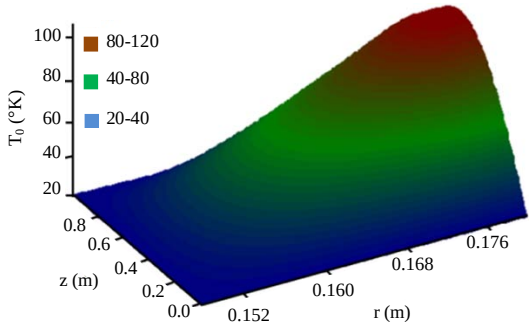

Fig. 2: The temperature distribution in the cylinder (ΔT = 80 °K)

temperature of only 30 °K and 57% in bearing layer of fiberglass. When analyzing the changes of normal stresses in the circumferential direction of the cylinder (Fig. 9) temperature rise 30 °K marked decrease in these stresses of 6% in the outer layer and 2% in the carrier layer. In this, thermal stress has little effect on the value of maximum pressure values for the region. Figures 11 and 12 show that, the transverse shift slightly depends on the magnitude of the thermal load but as known, even small stresses in the presence of the cross shear compressed or stretched transversal stresses. Figure 5 can cause delamination of the multilayer shell consideration.

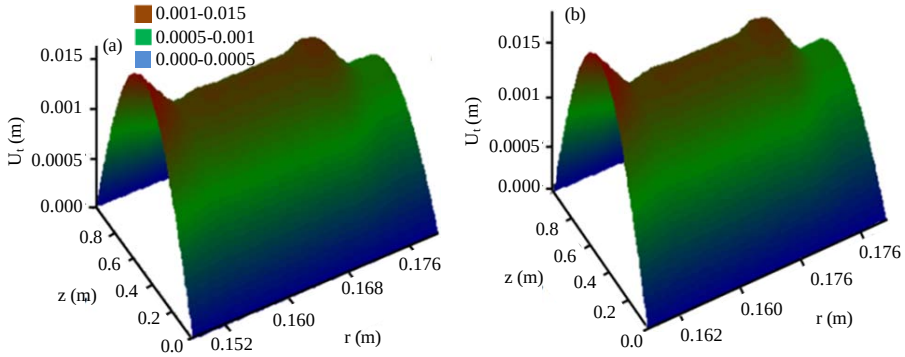

Fig. 3: Distribution of radial displacements in the cylinder (q_0 = 50 MPa): a) ΔT = 80 °K and b) ΔT = 50 °K

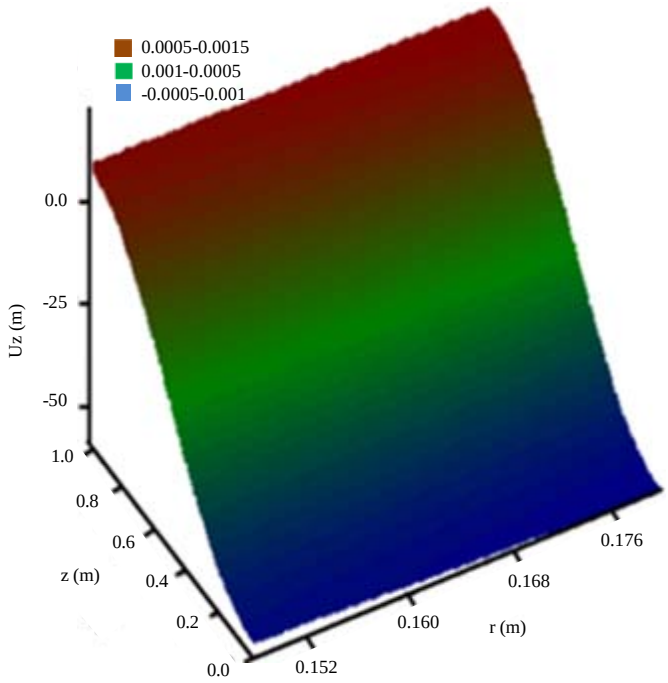

Fig. 4: Distribution of longitudinal displacements in the cylinder (q_0 = 50 MPa): a) ΔT = 80 °K and b) ΔT = 50 °K

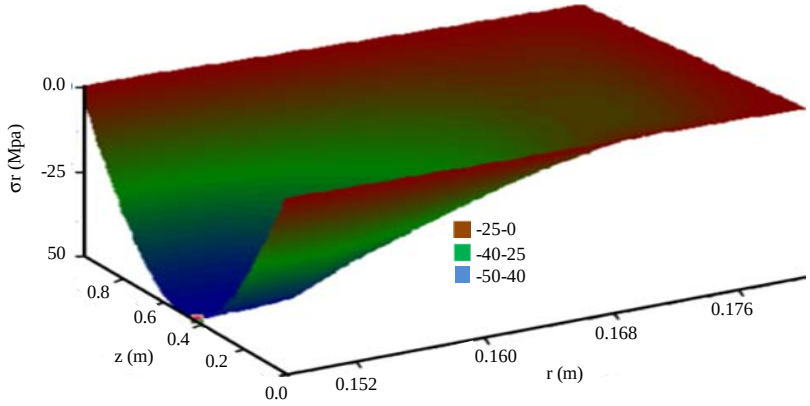

Fig. 5: Distribution of radiation stresses inside the cylinder (q_0 = 50 MPa, ΔT = 80 °K)

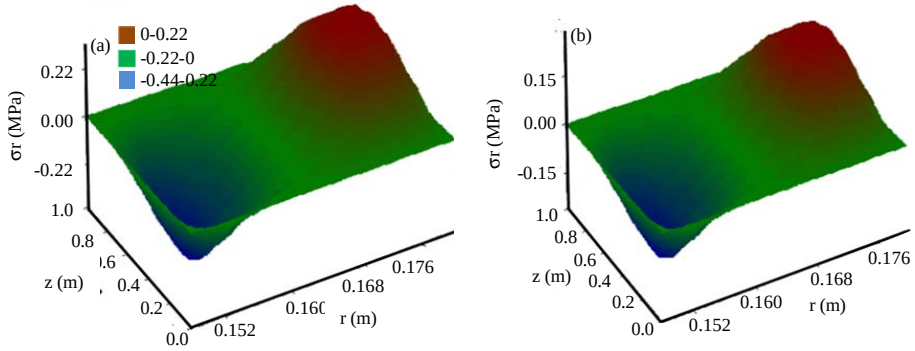

Fig. 6: Distribution of radial stresses inside the cylinder (q_0 = 0 MPa): a) ΔT = 80 °K and b) ΔT = 50 °K

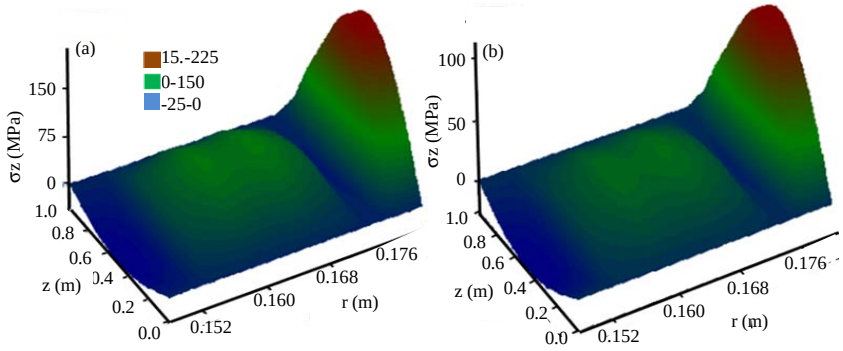

Fig. 7: Distribution of axial stresses in the cylinder (q_0 = 50 MPa): a) ΔT = 80 °K and b) ΔT = 50 °K

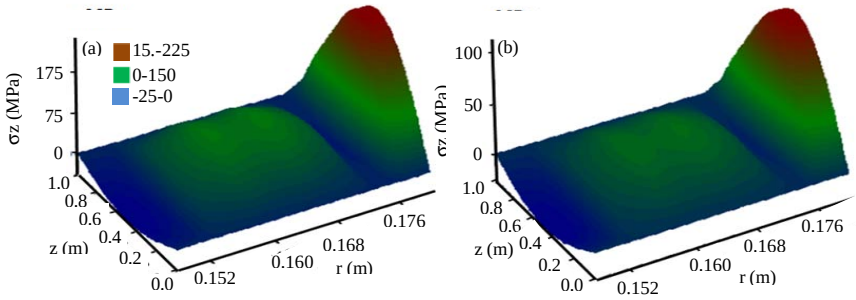

Fig. 8: Apportionment of axial stresses inside the cylinder (q_0 = 0 MPa): a) ΔT = 80 °K; b) ΔT = 50 °K

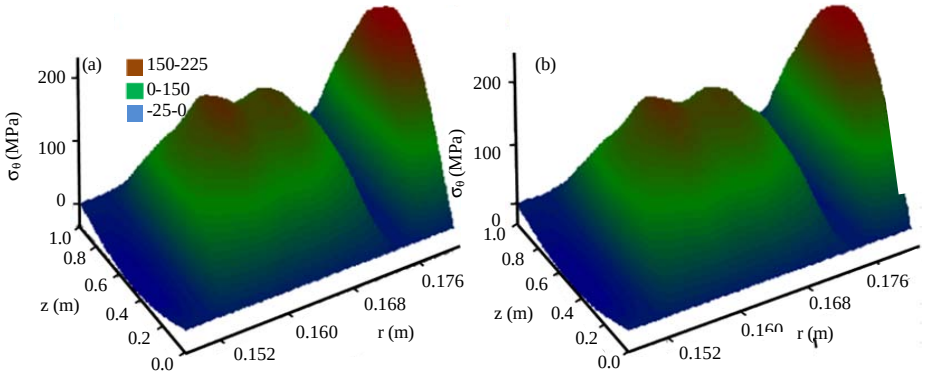

Fig. 9: Distribution of circumferential stress in the cylinder (q_0 = 50 MPa): a) ΔT = 80 °K and b) ΔT = 50 °K

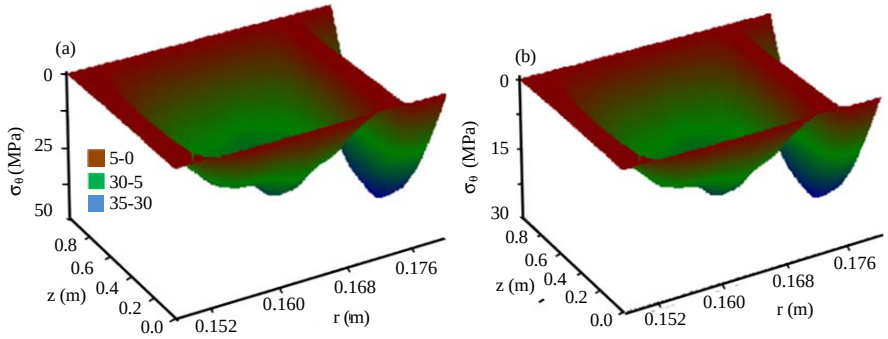

Fig. 10: Distribution of circumferential stress inside the cylinder (q_0 = 0 MPa): a) ΔT = 80 °K and b) ΔT = 50 °K

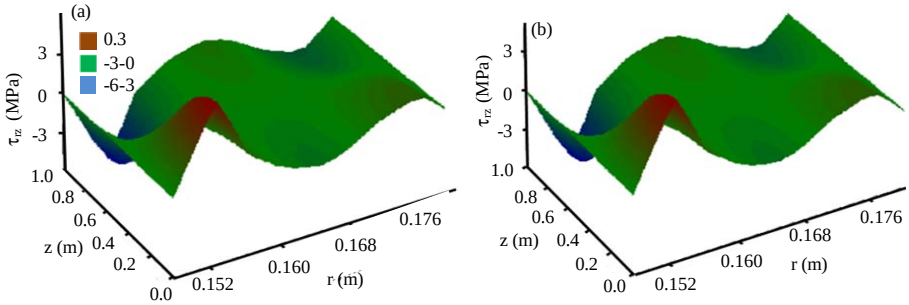

Fig. 11: Distribution of transverse shear stresses in cylinder (q_0 = 50 MPa): a) ΔT = 80 °K and b) ΔT = 50 °K

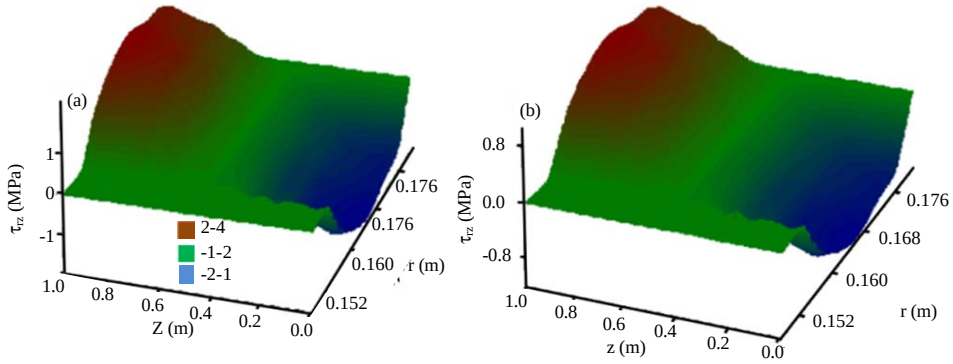

Fig. 12: Distribution of transverse shear stresses in cylinder (q_0 = 0 MPa): a) ΔT = 80 °K and b) ΔT = 50 °K

CONCLUSION

This study based on the discrete-structural theory, presents a study of stress-strain state of multilayered membranes under the impact of both static and thermal load, when taking into calculation the actual conditions and the amount of interaction between layers variation of contact stresses at the interlayer boundaries. A proposed algorithm to solve a class of problems considered here with estimations to assess the effect of physical and the mechanical characteristics of the individual layers on the thermo flexible strain state of inhomogeneous thickness of cylinders.

ACKNOWLEDGEMENTS

This research was backuped by Engineering Science Research Program through the Northern Technical University funded by the Ministry of Higher Education and Scientific Research/Republic of Iraq (No. 00333- 2017).

REFERENCES

Dasgupta, A. and K.H. Huang, 1997. A layer-wise analysis for free vibrations of thick composite spherical panels. J. Comp. Mater., 31: 658-671.

Herakovich, C.T., 1997. Mechanics of Fibrous Composites. John Wiley & Sons, Hoboken, New Jersey, USA., ISBN:9780471106364, Pages: 480.

Jabbari, M., S. Sohrabpour and M.R. Eslami, 2002. Mechanical and thermal stresses in a functionally graded hollow cylinder due to radially symmetric loads. Int. J. Pressure Vessels Piping, 79: 493-497.

Jabbari, M., S. Sohrabpour and M.R. Eslami, 2003. General solution for mechanical and thermal stresses in a functionally graded hollow cylinder due to nonaxisymmetric steady-state loads. J. Appl. Mech., 70: 111-118.

Jain, L.K. and Y.W. Mai, 1997. Stresses and deformations induced during manufacturing part I: Theoretical analysis of composite cylinders and shells. J. Comp. Mater., 31: 672-695.

Kim, K.S. and N. Noda, 2002a. A green's function approach to the deflection of a FGM plate under transient thermal loading. Arch. Appl. Mech., 72: 127-137.

Kim, K.S. and N. Noda, 2002b. Green's function approach to unsteady thermal stresses in an infinite hollow cylinder of functionally graded material. Acta Mech., 156: 145-161.

Lekhnitskij, S.G., 1977. Theory of the Elasticity of Anisotropic Bodies. National Academies of Sciences, Washington, USA., Pages: 416.

Obata, Y. and N. Noda, 1994. Steady thermal stresses in a hollow circular cylinder and a hollow sphere of a functionally gradient material. J. Thermal Stresses, 17: 471-487.

Ootao, Y. and Y. Tanigawa, 2000. Three-dimensional transient piezothermoelasticity in functionally graded rectangular plate bonded to a piezoelectric plate. Intl. J. Solids Struct., 37: 4377-4401.

Tanigawa, Y.O.Y., 1999. Three-dimensional transient thermal stresses of functionally graded rectangular plate due to partial heating. J. Therm. Stresses, 22: 35-55.

Tucker, R., P. Compston and P.Y.B. Jar, 2001. The effect of post-cure duration on the mode I interlinear fracture toughness of glass-fiber reinforced vinyl ester. Comp. Part A., 32: 129-134.